



Supporting Information

© Copyright Wiley-VCH Verlag GmbH & Co. KGaA, 69451 Weinheim, 2019

Towards New Robust Zn(II) Complexes for the Ring-Opening Polymerization of Lactide Under Industrially Relevant Conditions

Pascal M. Schäfer, Katja Dankhoff, Matthias Rothemund, Agnieszka N. Ksiazkiewicz, Andrij Pich, Rainer Schobert, Birgit Weber,* and Sonja Herres-Pawlis*© 2019 The Authors. Published by Wiley-VCH Verlag GmbH & Co. KGaA. This is an open access article under the terms of the Creative Commons Attribution Non-Commercial NoDerivs License, which permits use and distribution in any medium, provided the original work is properly cited, the use is non-commercial and no modifications or adaptations are made.

Table S1. Crystallographic data of **1** and **5**.

	1	5
CCDC	1901404	1901405
formula	C ₃₀ H ₃₆ N ₄ O ₁₀ Zn ₂	C ₄₀ H ₄₀ N ₄ O ₁₀ Zn ₂
sum formula	C ₃₀ H ₃₆ N ₄ O ₁₀ Zn ₂	C ₄₀ H ₄₀ N ₄ O ₁₀ Zn ₂
<i>M</i> g mol ⁻¹	743.41	867.50
crystal system	triclinic	monoclinic
space group	<i>P</i> -1	<i>P</i> 2 ₁ / <i>c</i>
crystal description	colourless plate	colourless plate
<i>a</i> / Å	9.4692(4)	16.9724(5)
<i>b</i> / Å	13.2391(6)	14.5261(5)
<i>c</i> / Å	13.1893(6)	17.2695(6)
<i>α</i> / °	96.547(4)	90
<i>β</i> / °	93.463(3)	115.352(2)
<i>γ</i> / °	106.449(4)	90
<i>V</i> / Å ³	1567.97(13)	3847.6(2)
<i>Z</i>	2	4
<i>ρ</i> _{calcd} / g cm ⁻³	1.575	1.498
<i>μ</i> / mm ⁻¹	1.593	1.311
crystal size/ mm	0.136×0.050×0.046	0.120×0.106×0.075
<i>F</i> (000)	768	1792
<i>T</i> / K	133(2)	133(2)
<i>λ</i> / Å	Mo-K _α 0.71073	Mo-K _α 0.71073
<i>θ</i> range/ °	2.09–28.47	1.9–28.1
Reflns. collected	8917	22994
Indep. reflns. (<i>R</i> _{int})	7320 (0.071)	8714 (0.033)
Parameters	415	505
<i>R</i> 1 (all data)	0.0464	0.0295
<i>wR</i> 2	0.1134	0.0662
Goof	0.89	0.94

Table S2. Selected bond lengths/ Å of **1** and **5**.

	Zn–N _{py}	Zn–N _{ax}	Zn–O _{ax}	Zn–O53	Zn2–O51	Zn1–O52	O51–C51	O52–C51	O53–C53	O54–C53
1	2.134(3) 2.159(3)	2.031(3) 2.021(3)	2.059(3) 2.054(3)	2.024(3) 2.035(3)	2.031(3)	1.978(3)	1.257(5)	1.270(5)	1.311(5)	1.222(5)
5	2.1189(11) 2.1662(19)	2.0330(15) 2.0424(16)	2.0435(15) 2.0500(16)	2.0396(13) 2.0499(13)	2.0086(16)	1.9708(15)	1.250(2)	1.263(2)	1.307(2)	1.221(2)

Table S3. Hydrogen bonds and angles of **1** and **5**.

		D–H/Å	H···A/Å	D···A/Å	D–H···A/°
1	C14–H14···O54 ^a	0.95	2.34	3.140(5)	142
5	C13–H13···O33 ^b	0.95	2.43	3.287(3)	150
	C14–H14···O54 ^b	0.95	2.43	3.309(3)	154
	C27–H27A···O32 ^c	0.99	2.57	3.205(3)	122
	C33–H33···O54 ^d	0.95	2.46	3.175(3)	132
	C44–H44···O51 ^e	0.95	2.50	3.393(3)	157
	C52–H52B···O12 ^f	0.98	2.52	3.454(3)	160

a: -1+x, y, z; b: x, 1/2-y, 1/2+z; c: 1+x, y, 1+z; d: 2-x, -y, 1-z; e: 1-x, -y, 1-z; f: 2-x, -y, 2-z.

Table S4. Summary of the C–H···π interactions of **1** and **5**.

		C _g	H···C _g /Å	X–H···C _g /°	X···C _g /Å
1	C6–H6B	Zn2–N31–C35–C36–N32 ^a	2.769	147	3.626(4)
	C36–H36A	Zn1–N11–C15–C16–N12 ^b	2.95	135	3.718(4)
	C42–H42B	Zn2–O31–C39–C38–C37–N32 ^c	2.68	138	3.479(5)
5	C32–H32	C20–C21–C22–C23–C24–C25 ^d	2.67	142	3.467(2)
	C16–H16B	Zn1–O11–C19–C18–C17–N12 ^e	2.48	153	3.388(2)
	C44–H44	Zn2–O31–C39–C38–C37–N32 ^f	2.85	126	3.493(2)

a: -1+x, y, z; b: 1+x, y, z; c: 2-x, -y, 1-z; d: x, y, z; e: 2-x, -y, 2-z; f: 1-x, -y, 1-z.

Table S5. Selected distances and angles of the π - π and M- π interactions of **1** and **5**. $C_g(I)$ is the centroid of the ring number I, α is the dihedral angle between the rings, β is the angle between the vector $C_g(I) \rightarrow C_g(J)$ and the normal to ring I, γ is the angle between the vector $C_g(I) \rightarrow C_g(J)$ and the normal to ring J.

	$C_g(I)$	$C_g(J)$	$C_g-C_g/\text{\AA}$	$\alpha/^\circ$	$\beta/^\circ$	$\gamma/^\circ$
1	N31-C31-C32-C33-C34-C35	N31-C31-C32-C33-C34-C35 ^a	3.721(2)	0.00(19)	22.1	22.1
5	N31-C31-C32-C33-C34-C35	N31-C31-C32-C33-C34-C35 ^b	3.4814(12)	0.00(10)	18.0	18.0

a: 2-x, -y, 2-z; b: 2-x, -y, 1-z.

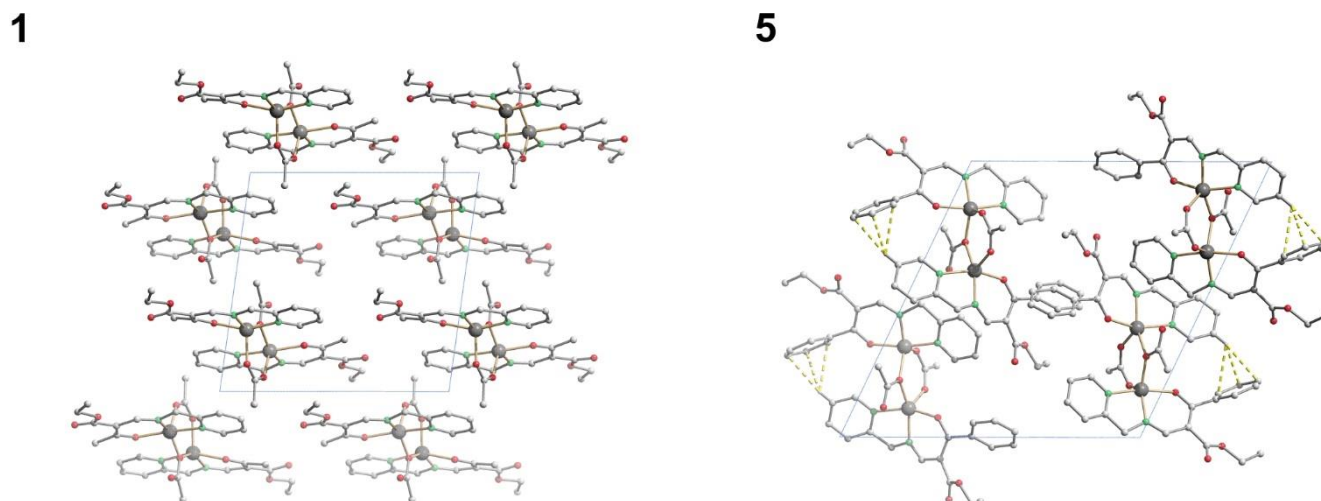


Figure S1. Molecular packing of **1** (left, along [100]) and **5** (right, along [010]). Discussed C-H \cdots π interactions of **5** are drawn as yellow, dashed lines. Hydrogen atoms not involved in intermolecular interactions were omitted for clarity.

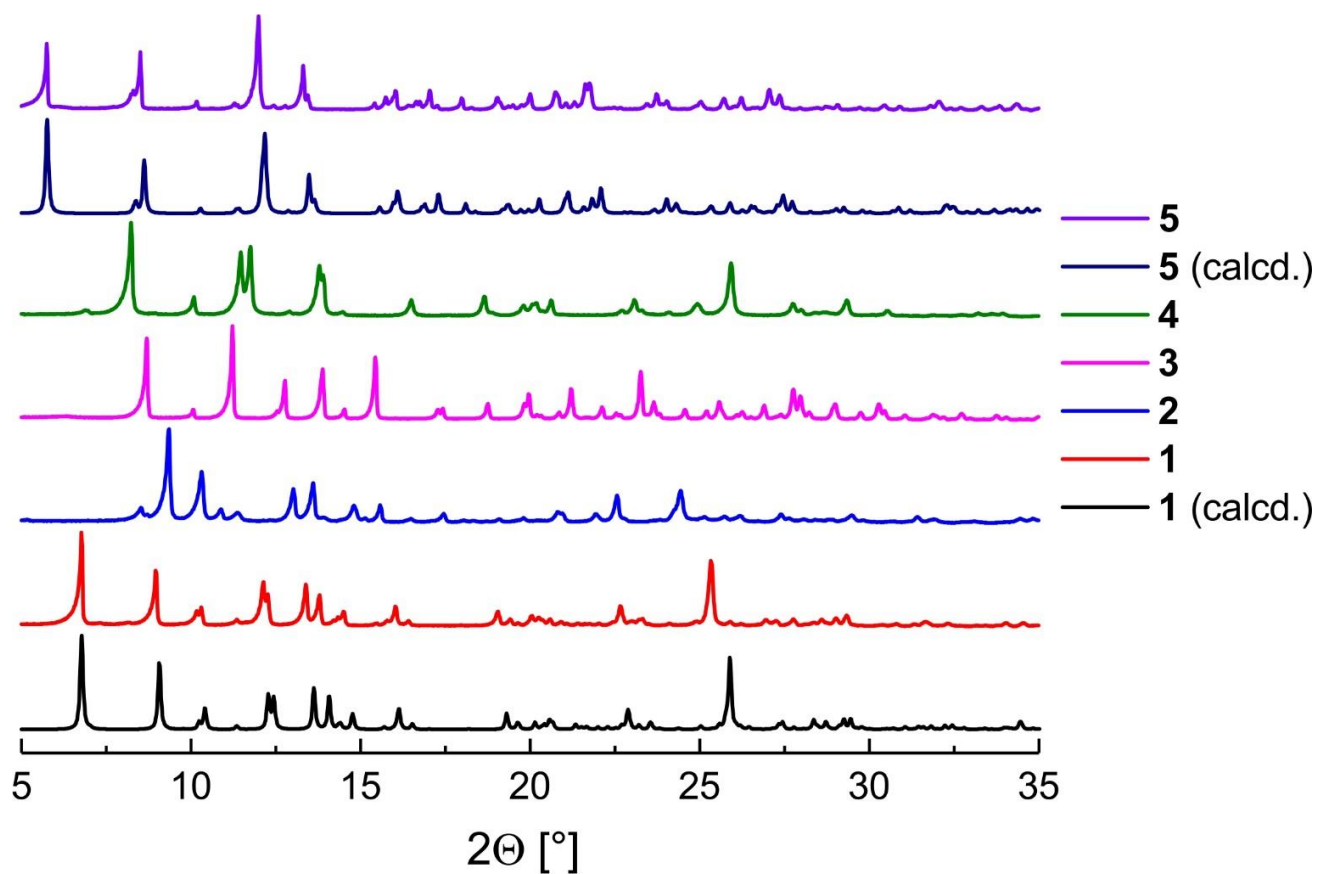


Figure S2. Powder X-ray diffraction patterns of 1–5, measured and calculated. The calculated patterns were obtained at 133 K, the measured ones at room temperature.

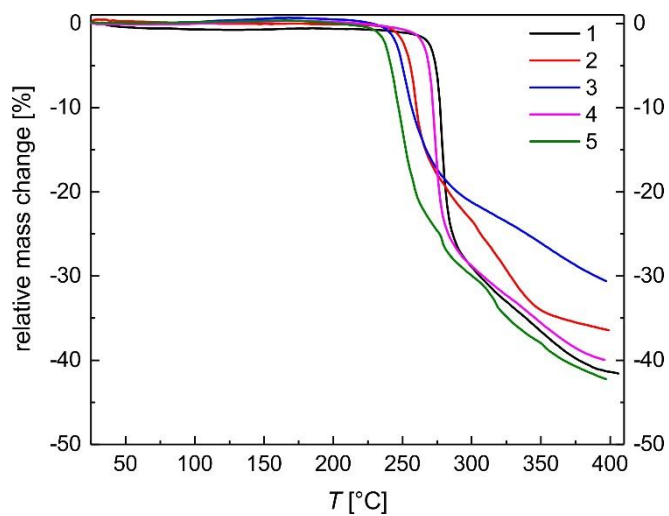


Figure S4. TGA measurements of complexes 1–5.

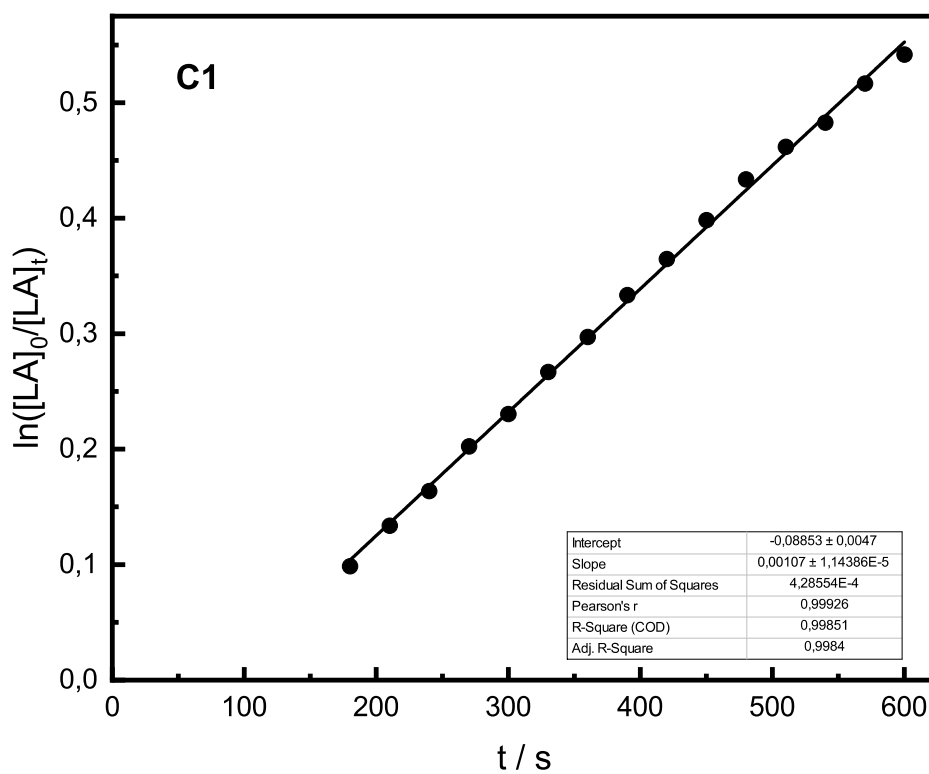


Figure S5. Semi-logarithmic plot of the polymerization of non-purified *rac*-LA with 1 $[M]/[I] = 500:1$, 150 °C, 260 rpm, conversion determined by *in situ* Raman spectroscopy.

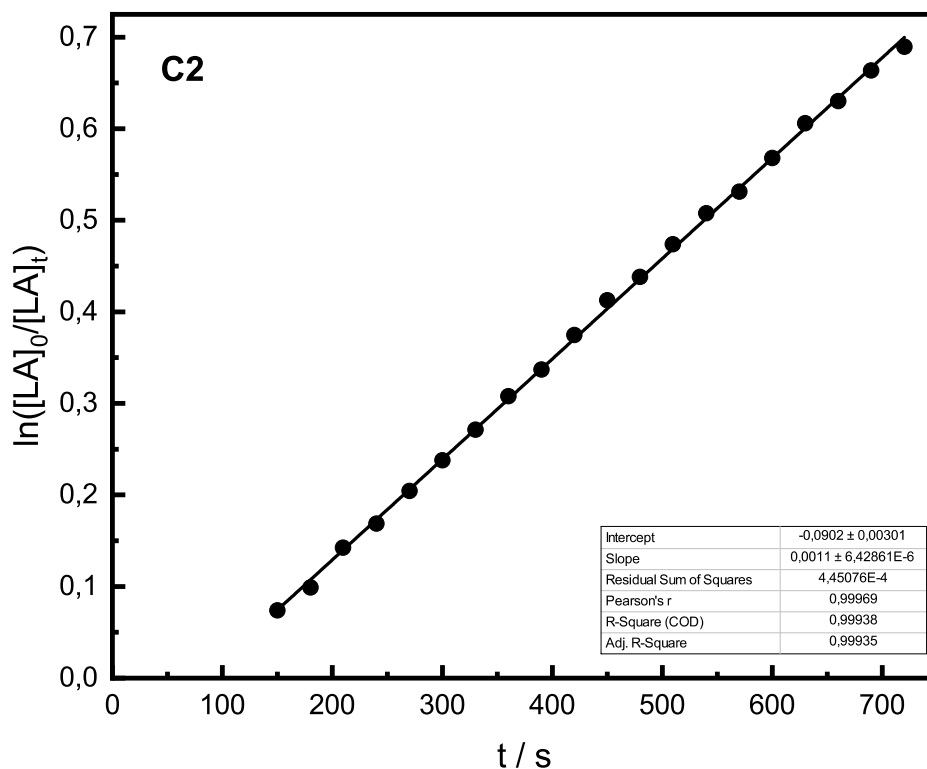


Figure S6. Semi-logarithmic plot of the polymerization of non-purified *rac*-LA with **2** [M]/[I] = 500:1, 150 °C, 260 rpm, conversion determined by *in situ* Raman spectroscopy.

Table S7. Polymerization data for *rac*-LA with catalyst **2**.

[M]/[I]	k_{app} (s ⁻¹) ^[b]	time (min)	conv. (%) ^[c]	$M_{n,theo}$ (g mol ⁻¹)	M_n (g mol ⁻¹) ^[d]	<i>PD</i>
500	1.14 × 10 ⁻³	25	62	45 000	65 000	1.5
625	8.60 × 10 ⁻⁴	30	78	70 000	54 000	1.8
1000	4.22 × 10 ⁻⁴	27	65	94 000	81 000	1.4
1500	2.23 × 10 ⁻⁴	61	57	123 000	43 000	1.8
2000	1.28 × 10 ⁻⁴	112	56	161 000	21 000	2.2

[a] Conditions: 150 °C, solvent free, non-purified technical grade *rac*-LA. [b] Determined from the slope of the plots of ln([LA]₀/[LA]_t) versus time. [c] As determined by ¹H NMR spectroscopy. [d] Determined by GPC (in THF), $M_{n,theo}$: 72 000 g mol⁻¹ for 100% conversion.

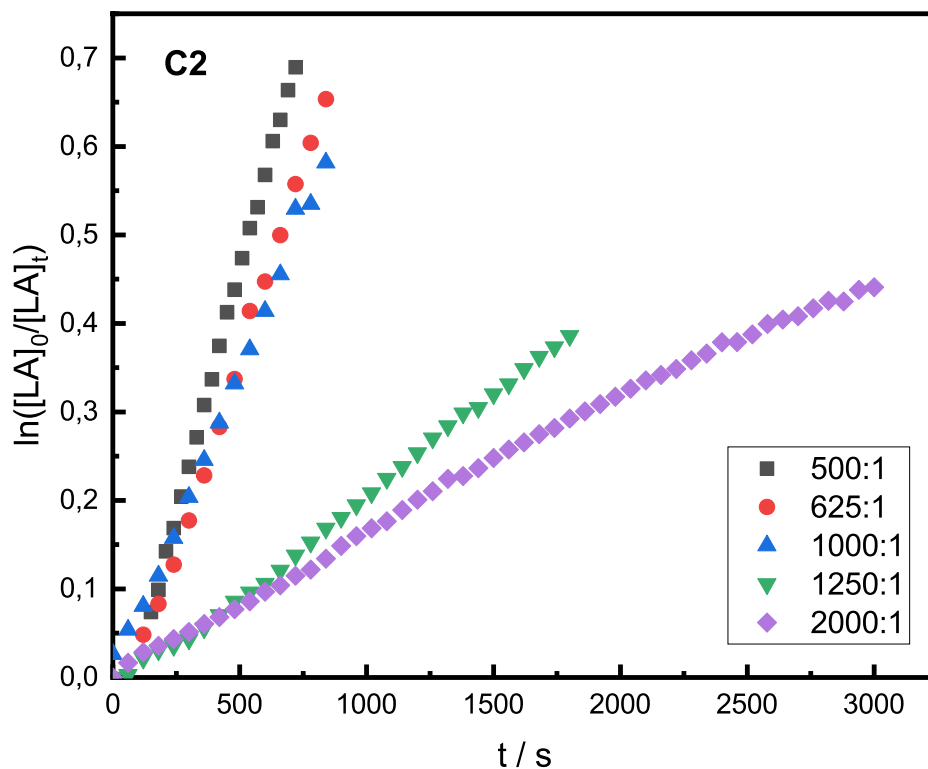


Figure S7. Semi-logarithmic plot of the polymerization of non-purified *rac*-LA with **2** $[M]/[I] = 500:1$ ($k_{app} =$), $[M]/[I] = 625:1$ ($k_{app} =$), $[M]/[I] = 1000:1$ ($k_{app} =$), $[M]/[I] = 1250:1$ ($k_{app} =$), $[M]/[I] = 2000:1$ ($k_{app} =$), 150 °C, 260 rpm, conversion determined by *in situ* Raman spectroscopy.

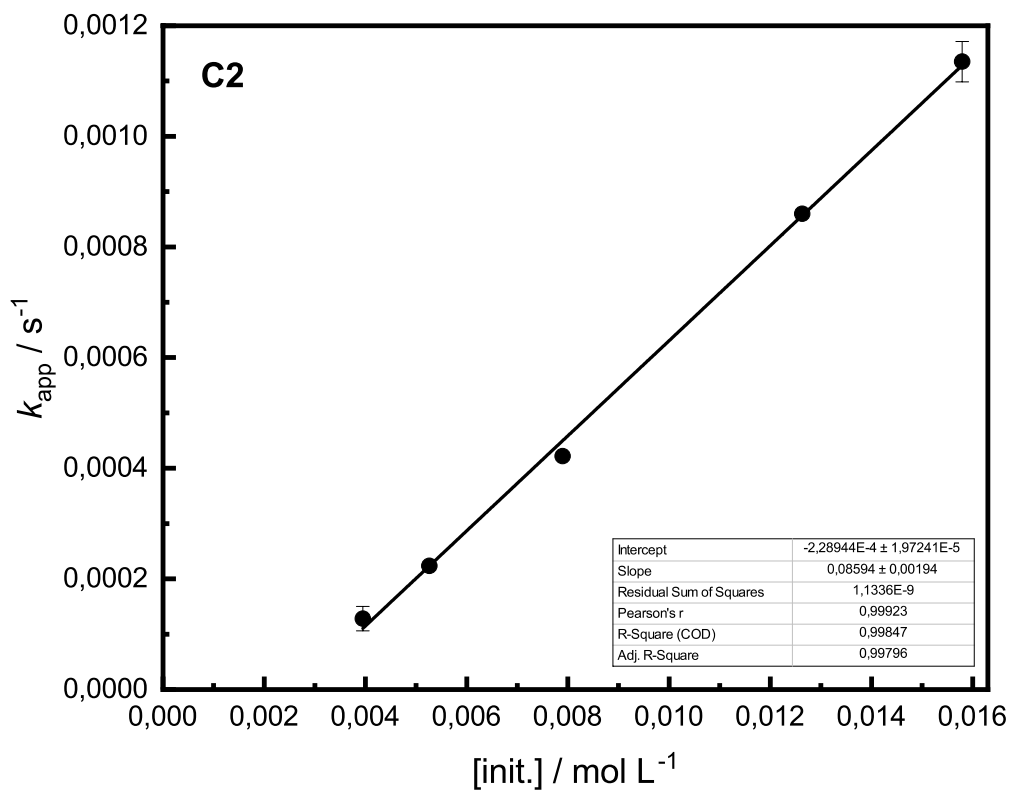


Figure S8. Plot of k_{app} versus $[init.]$ for **2**. Conditions: *rac*-LA, 150 °C, 260 rpm, non-purified; $[M]/[I] = 500:1$, 625:1, 1000:1, 1500:1, 2000:1.

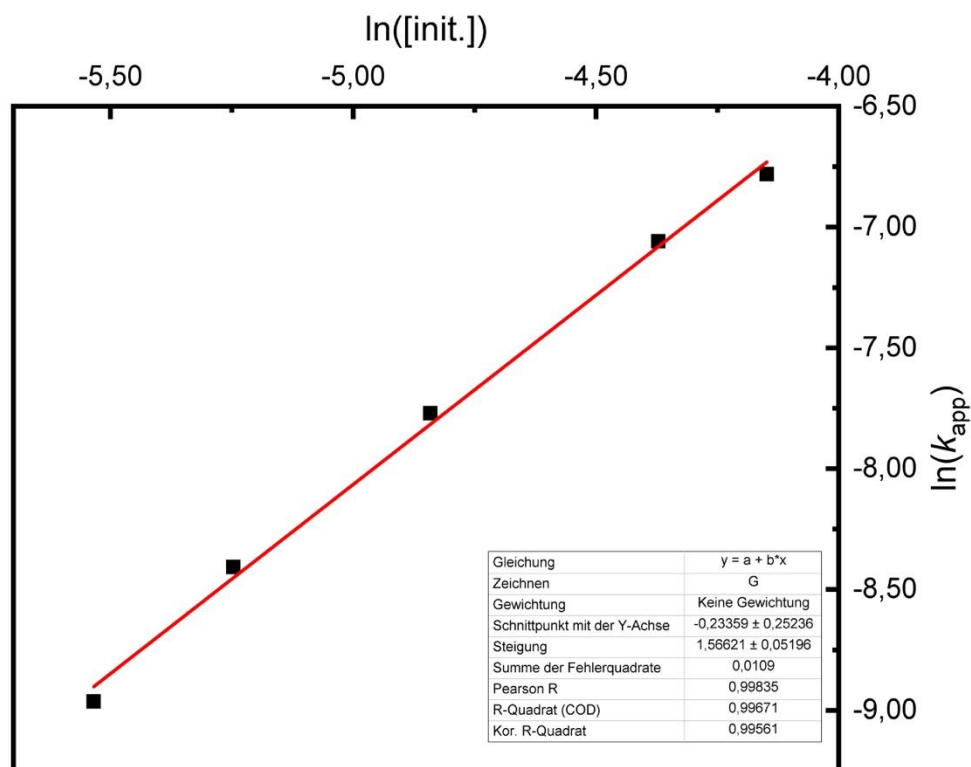


Figure S9. Logarithmic plot of $\ln(k_{app})$ versus $\ln([init.])$ for the polymerization of non-purified *rac*-LA with 4 $[M]/[I] = 500:1$, 150 °C, 260 rpm.

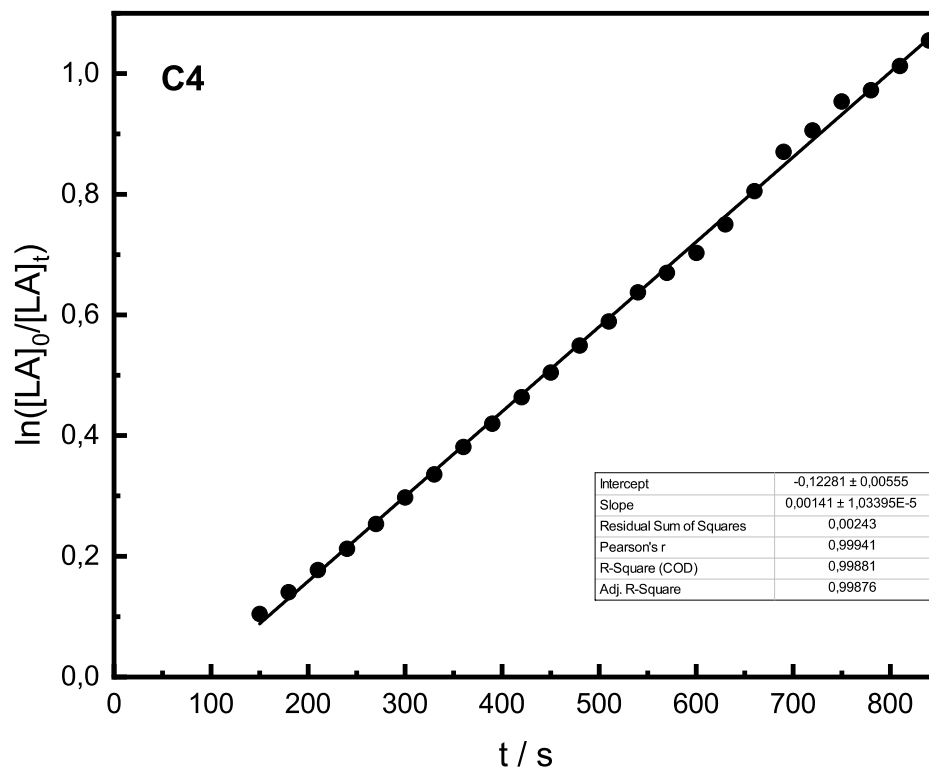


Figure S10. Semi-logarithmic plot of the polymerization of non-purified *rac*-LA with 4 $[M]/[I] = 500:1$, 150 °C, 260 rpm, conversion determined by *in situ* Raman spectroscopy.

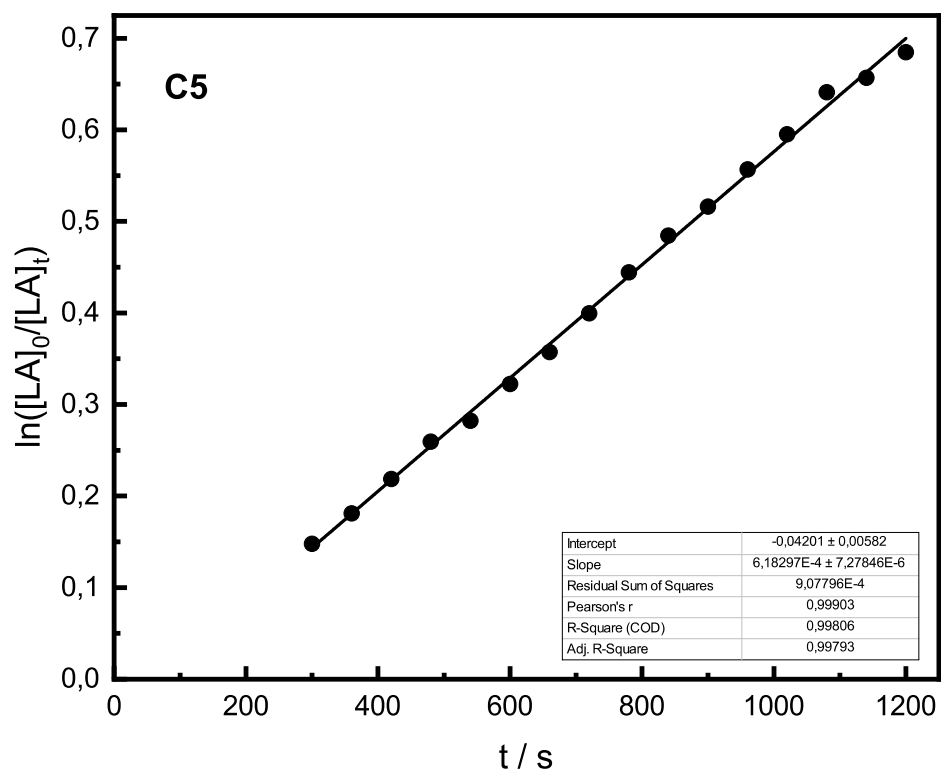


Figure S11. Semi-logarithmic plot of the polymerization of non-purified *rac*-LA with 5 [M]/[I] = 500:1, 150 °C, 260 rpm, conversion determined by *in situ* Raman spectroscopy.

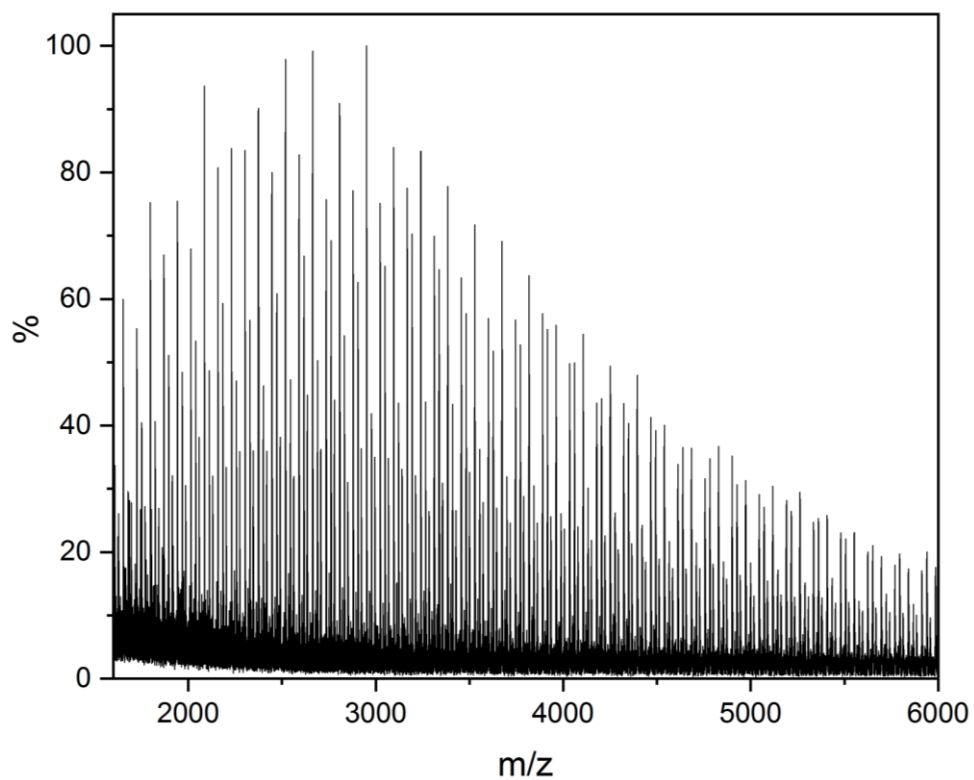


Figure S12. Stack of MALDI-ToF spectra obtained for a polymerisation with 4 [M]/[I] = 70:1, 150 °C, 260 rpm, *rac*-LA.

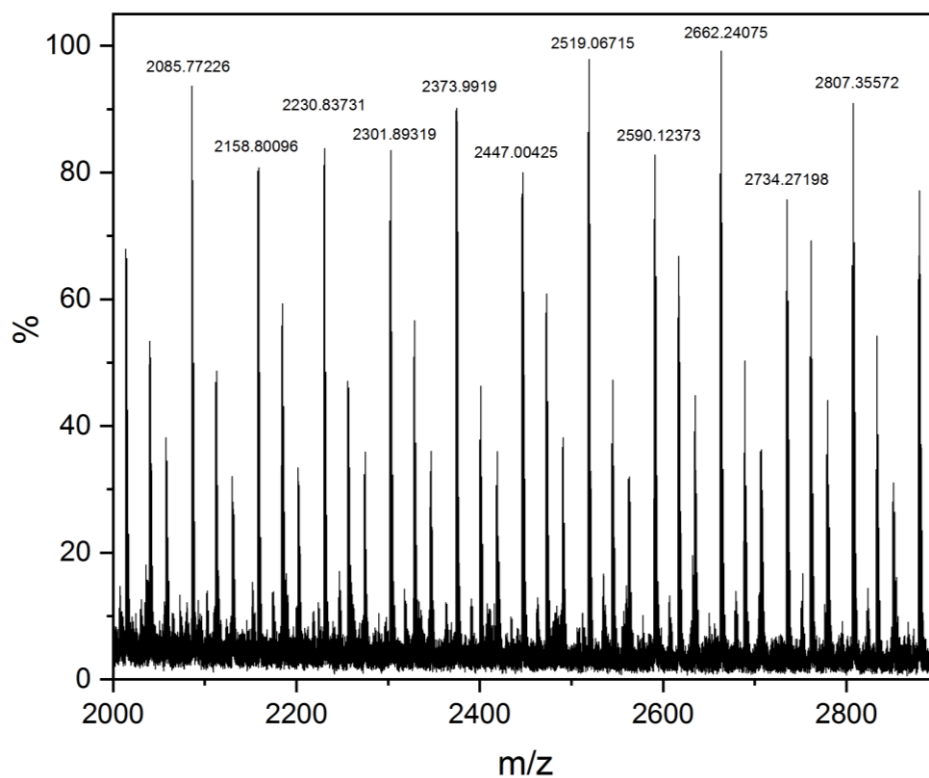


Figure S13. Stack of MALDI-ToF spectra obtained for a polymerisation with **4** [M]/[I] = 70:1, 150 °C, 260 rpm, *rac*-LA. For m/z 2807.35572:

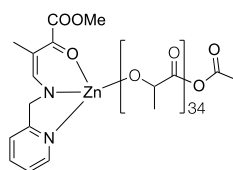
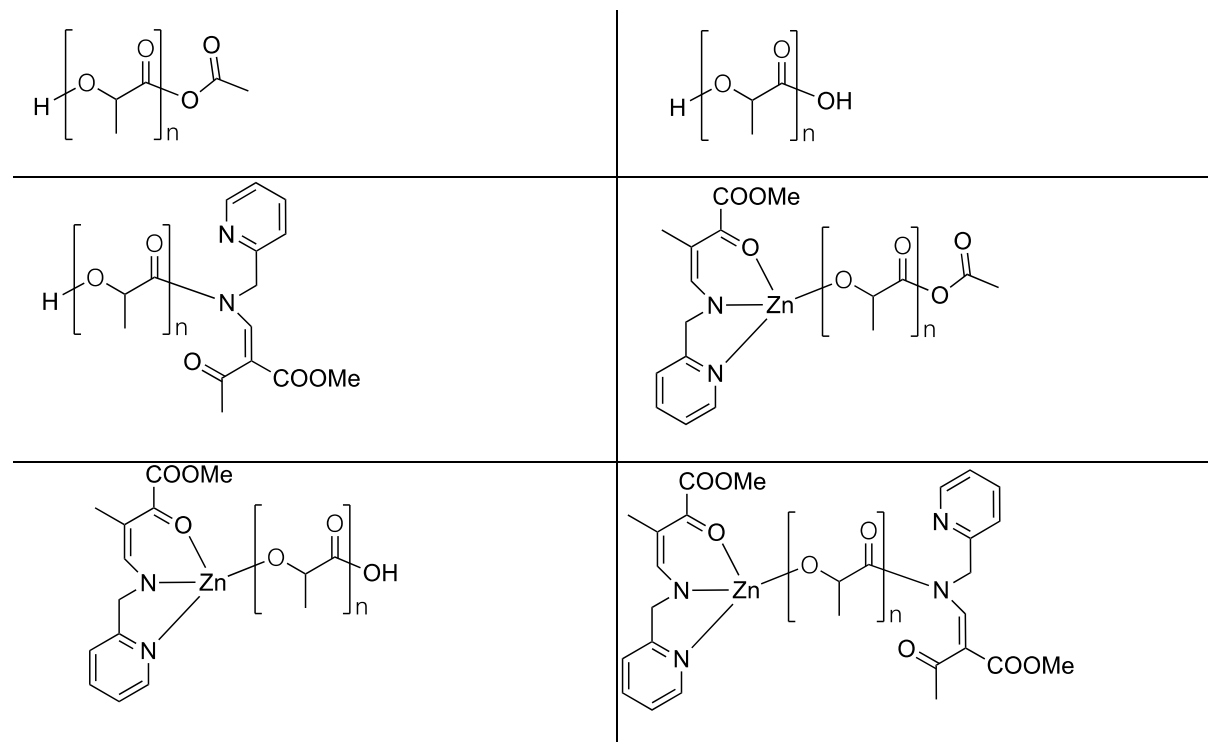


Table S8. Possible end-groups for the obtained polymer initiated by **4** [M]/[I] = 70:1, 150 °C, 260 rpm, *rac*-LA.



Results of the MALDI-ToF analysis for all series of the spectrum:

Ligand-Zn-PLA: 26.77%
Ligand-PLA: 10.59%
Acetate-PLA: 22.94%
OH: 10.53%
H: 17.29%

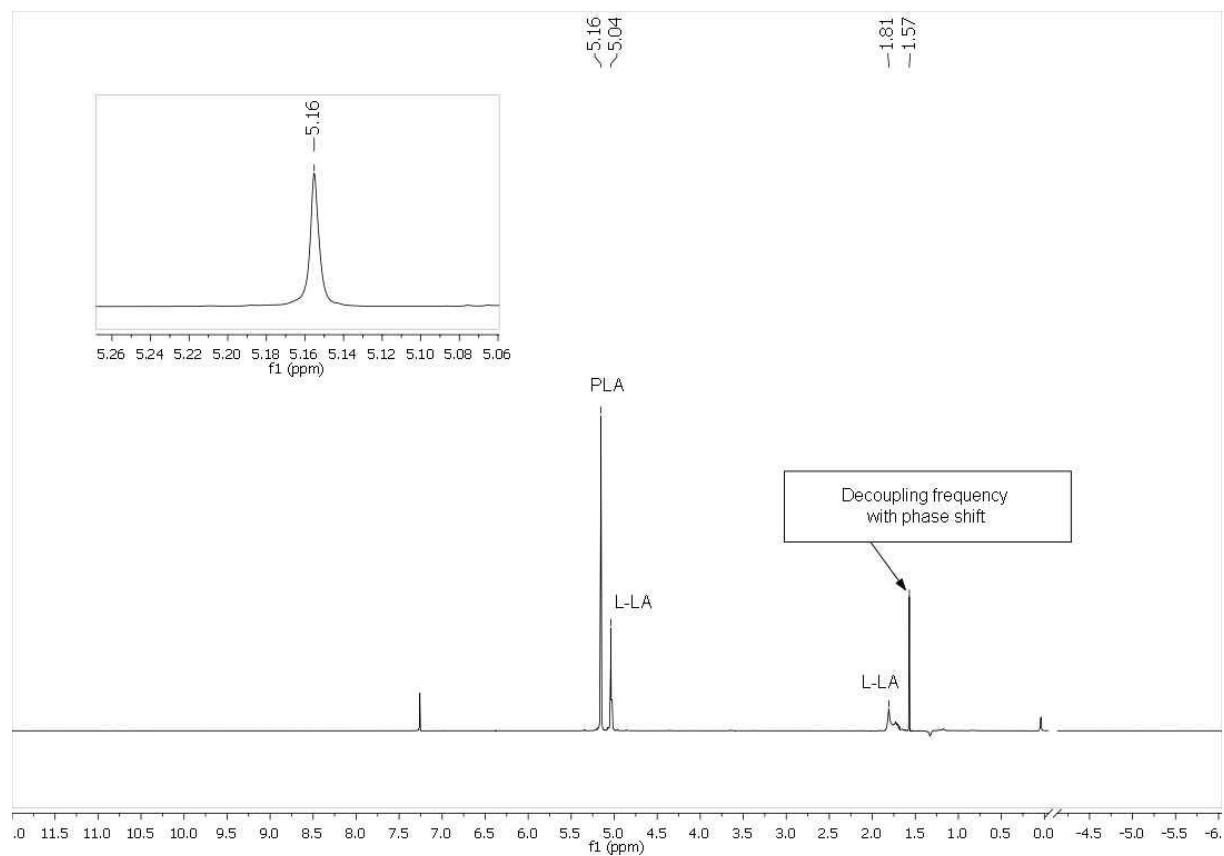


Figure S14. Homonuclear decoupled ¹H NMR spectrum (CDCl₃, 400 MHz) of PLA prepared by polymerization of L-lactide with **2** at 150 °C.